THE OFFICIAL MAGAZINE OF THE OCEANOGRAPHY SOCIETY

Oceanography

CITATION

Reverdin, G., S. Morisset, L. Marié, D. Bourras, G. Sutherland, B. Ward, J. Salvador, J. Font, Y. Cuypers, L. Centurioni, V. Hormann, N. Koldziejczyk, J. Boutin, F. D'Ovidio, F. Nencioli, N. Martin, D. Diverres, G. Alory, and R. Lumpkin. 2015. Surface salinity in the North Atlantic subtropical gyre during the STRASSE/SPURS summer 2012 cruise. *Oceanography* 28(1):114–123, http://dx.doi.org/10.5670/oceanog.2015.09.

DOI

http://dx.doi.org/10.5670/oceanog.2015.09

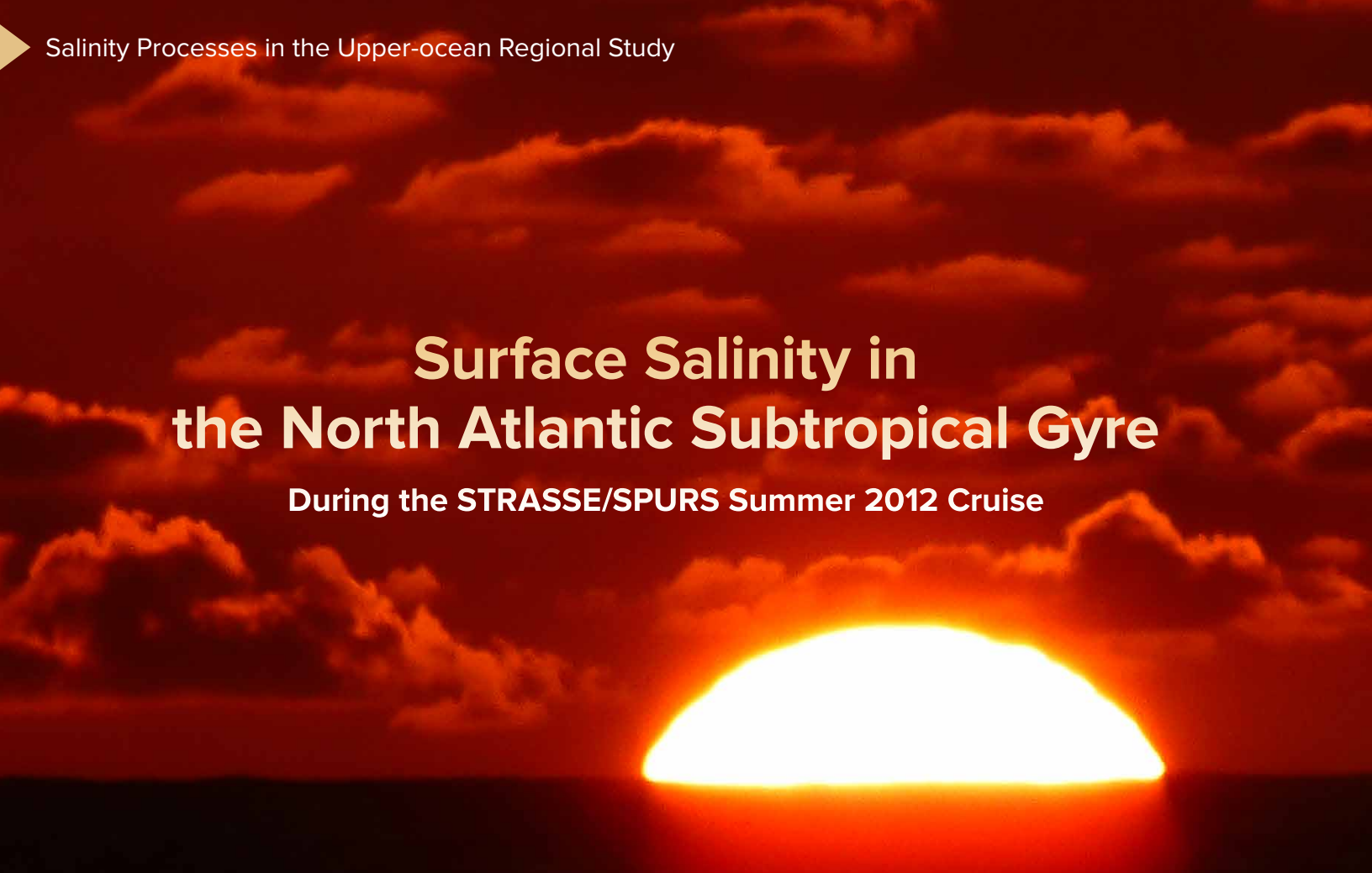

Surface Salinity in the North Atlantic Subtropical Gyre

During the STRASSE/SPURS Summer 2012 Cruise

By Gilles Reverdin, Simon Morisset, Louis Marié, Denis Bourras, Graigory Sutherland, Brian Ward, Joaquín Salvador, Jordi Font, Yannis Cuypers, Luca Centurioni, Verena Hormann, Nicolas Koldziejczyk, Jacqueline Boutin, Francesco D'Ovidio, Francesco Nencioli, Nicolas Martin, Denis Diverres, Gaël Alory, and Rick Lumpkin

ABSTRACT. We investigated a 100 × 100 km high-salinity region of the North Atlantic subtropical gyre during the Sub-Tropical Atlantic Surface Salinity Experiment/Salinity Processes in the Upper-ocean Regional Study (STRASSE/SPURS) cruise from August 21, 2012, to September 9, 2012. Results showed great variability in sea surface salinity (SSS; over 0.3 psu) in the mesoscale, over 7 cm of total evaporation, and little diapycnal mixing below 36 m depth, the deepest mixed layers encountered. Strong currents in the southwestern part of the domain, and the penetration of freshwater, suggest that advection contributed greatly to salinity evolution. However, it was further observed that a smaller cyclonic structure tucked between the high SSS band and the strongest currents contributed to the transport of high SSS water along a narrow front. Cross-frontal transport by mixing is also a possible cause of summertime reduction of SSS. The observed structure was also responsible for significant southward salt transport over more than 200 km.

INTRODUCTION

During boreal summer, there are moderate to weak winds, a seasonal surface salinity maximum, and large near-surface stratification at the center of the North Atlantic subtropical gyre (Boyer and Levitus, 2002; de Boyer-Montégut et al., 2004). Mesoscale structures such as eddies in this region are expected to contribute to lateral mixing in the surface salinity maximum region. Kolodziejczyk et al. (2014a) investigated surface temperature and salinity and suggest that salinity features dominate surface density spatial variability during boreal summer, with typical amplitudes of the order of 0.1 psu at scales smaller than 200 km. There was weak correlation between temperature and salinity variability in this region and during this season. Kolodziejczyk et al. (2014b) indicated that summer 2012 conditions in the salinity maximum were influenced by anomalously salty subsurface waters that originated farther to the northeast at the end of the previous winter and by locally salty surface waters.

Horizontal stirring of a tracer by mesoscale eddies is associated with a cascade of variance toward smallest horizontal scales (Capet et al., 2008). Thus, stirring would contribute to an increase over time in horizontal spatial variability of the tracer and a decrease in spatial scales during summer, a season characterized by shallow mixed layers and fairly regular atmospheric forcing, as well as weak eddy activity. On the other hand, other processes associated with fronts, vertical mixing or transports, air-sea fluxes, and mixed-layer processes could limit this transfer of variance through horizontal stirring. We need to investigate which processes are active. In particular, are they similar to what was found in areas of higher mesoscale activity/energy (Mahadevan and Tandon, 2006)? Does wind play a role in cross-frontal transport (e.g., Thomas and Lee, 2005, or Hosegood et al., 2013)?

The French STRASSE (Sub-Tropical Atlantic Surface Salinity Experiment) cruise investigated the spatial distribution of surface salinity over 20 days during the summer of 2012 (August 21–September 9) in a small area of the North Atlantic subtropical gyre during the Salinity Processes in the Upper-ocean Regional Study (SPURS). The goal of STRASSE was to answer three questions:

- Is there evidence of salinity structures resulting from lateral stirring by eddies?
- What is the coherence between temperature and salinity surface structures, and are there any subsurface structures that mirror the surface structures?
- What are the smallest filament scales and what is the dissipation process of the smallest structures? Are they related to cross-frontal processes or do they involve air-sea fluxes?

Mid-August sea surface salinity (SSS) maps (Figure 1a,b) derived from Aquarius (Lagerloef et al., 2012; Yueh et al., 2014) and Soil Moisture and Ocean Salinity (SMOS) (Boutin et al., 2012; Font et al., 2013) data show a salty band around and to the east of an anticyclonic structure centered near 25.5°N, 36.3°W (A1 in Figure 1). The SMOS product (Figure 1c) also suggests that the water in the core of A1 is rather fresh and is fed by water from further south. Some of the structures with largest SSS near 25°–26°N are found both in SMOS and Aquarius-derived products, although details differ between the two, with the Aquarius product presenting less spatial variability, but the data are probably also less noisy (Hernandez et al., 2014; Yueh et al., 2014).

The possibility of encountering surface salinity filaments in this region is also explored with semi-Lagrangian and Lyapunov exponent tools (d'Ovidio et al., 2009), based on a salinity field advected in mesoscale currents derived by Ssalto/Duacs altimetry processing. Tests done on large-scale SSS maps with the In Situ Analysis System (ISAS) for August 2012 (Gaillard, 2012) show some features that are fairly similar to those in the satellite-derived maps (Figure 1c). In longer simulations, the very large pool of freshwater near 27.5°N, 36°W extended further south; filaments reached the vicinity of the STRASSE box near 26°N, 35°W by late August and were associated with development of a saltier band to the west of it that was oriented northwest-southeast. The simulations were supported by a 25 km wide salty structure observed by MN *Toucan* near 26.2°N, 35.6°W on August 15. Thus, both the quasi-Lagrangian tests and these satellite products indicate salt structures that have the potential for frontal development in the region near 26°N, 35°–36°W.

Based on this information, we selected a slightly north-south elongated area from 25.5°–26.5°N and 35°–36°W for our study. We deployed autonomous instruments during an initial 14-hour criss-cross transect and conducted a hydrographic survey. These operations were followed by three three-day stations that tracked drifter clusters in order to investigate frontal structures near large surface salinity filaments.

The area near 26°N, 35.5°W received little rain during the surveys. For two days during the in situ survey period, we measured strong vertical haline stratification of up to 0.1 psu in the top 2 m of the water column caused by evaporation during very weak winds (Asher et al., 2014). Otherwise, the winds were weak to moderate, not exceeding 10 m s^{-1}. Large daily insulation (except on August 27) regularly induced a strong daily cycle in temperature stratification and vertical mixing that was investigated by Sutherland et al. (2014). During those days, instrumented wave riders measured a small daily SSS cycle of 0.01 psu (Reverdin et al., 2013).

INSTRUMENTATION

Air-sea fluxes were estimated by combining data from the different meteorological packages on R/V *Thalassa* with ship-mast winds that were corrected by comparing those data with nearby wind measurements recorded during deployments of the autonomous instrumented platform Ocarina (Bourras et al., 2014). Comparison of humidity measurements from three instruments indicated absolute accuracy of corrected relative humidity on the order of 1%. An additional error—possibly of a similar magnitude—is caused by uncertainty in the equivalent height of the humidity measurements due to flow distortions by the ship. Evaporation, latent and sensible heat, and wind stress were then estimated using the COARE2.5b package (Fairall et al., 1996).

The mesoscale coverage combined spatial surveys within the domain 25.5°–26.5°N, 35°–36°W and Lagrangian time series. R/V *Thalassa* largely provided the spatial coverage, either by conducting conductivity-temperature-depth (CTD) casts or by towing an undulating Scanfish MKII (product of GMI, Denmark) vehicle with Sea-Bird CTD sensors from the surface to 100 m, as well as by taking continuous temperature and salinity (T/S) and other online water measurements for water pumped at 3.5 m depth. Two shallow gliders were also deployed on August 21 (until early October) and on August 22 (for five days). Those data were corrected based on nearby CTD casts and with resulting uncertainties in salinity of less than 0.01 psu, except in the presence of large vertical temperature gradients. In addition, an array of GPS-tracked or Argos-tracked drifters drogued at 15 m depth was deployed to measure either just temperature (10 drifters) or temperature and salinity (15 drifters) to contribute to the mesoscale sampling. A few additional T/S profiles were collected from two dedicated Argo floats along with surface T/S measurements from an autonomous sailing vessel during three days, and one surface T/S section was provided by the thermosalinograph onboard MN *Toucan*, which crossed the area on August 28.

At the beginning of each long station (three days duration), at least five Surface Velocity Program (SVP) drifters drogued at 15 m depth were deployed to measure temperature and salinity (SVPS), most of them along with a Surpact wave rider (Reverdin et al., 2013). The drifters were initially deployed within a 1 km radius. During daytime, the ship remained close to the drifters and deployed other platforms (the Air-Sea Interaction Profiler [ASIP], Trefle [a drifter drogued at 50 m], and Ocarina). Trefle measured sea state and recorded current profiles at 1 m depth and at 1 min resolution from 3 m down to about 100 m depth. Positions of Trefle and the SVP drifters differed at times, in particular, during Station 3, due to vertical shear of horizontal currents associated particularly with near-inertial oscillations. The autonomous profiler ASIP (Ward et al., 2014) was also regularly deployed for durations of one to two days (Sutherland et al., 2014). It measured T/S and recorded turbulence profiles (from shear probes) from near the surface to about 60 m. At night, the ship conducted spatial Scanfish CTD surveys within 10 km of the drifters.

Drifter velocities usually showed large near-inertial oscillations, which were filtered by a 26 h running average.

TIME SERIES

The in situ data were gridded and then interpolated to estimate an average time series of sea surface temperature (SST) and SSS in the STRASSE domain; we removed an estimated daily cycle so that the daily data represent morning conditions (Figure 2a). We estimated daily wind stress and evaporation (latent heat flux) from the ship

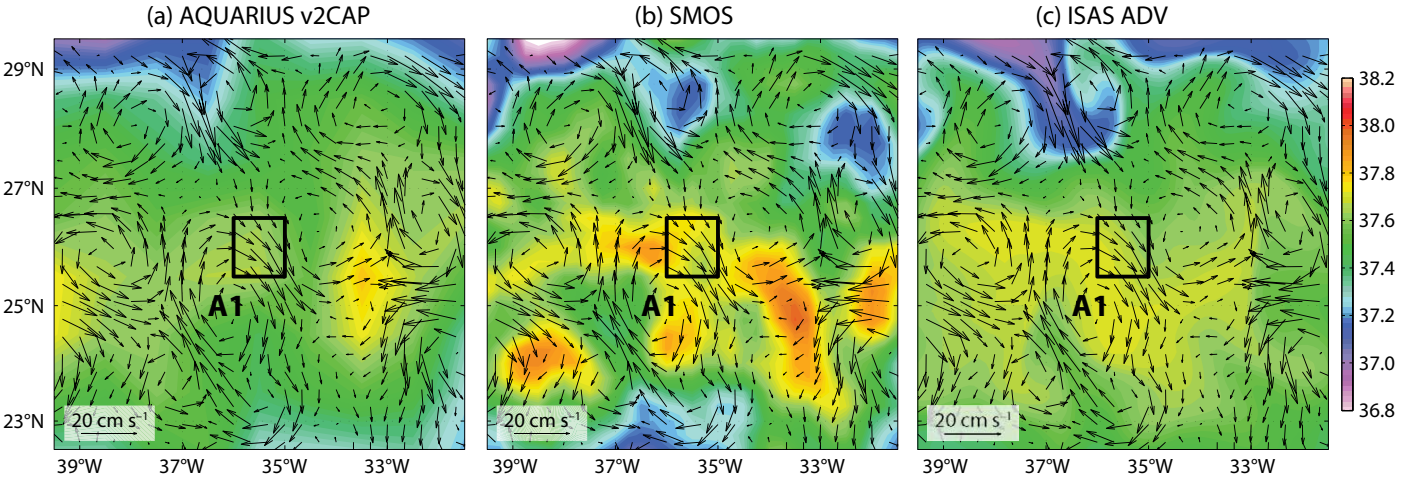

FIGURE 1. Mesoscale fields in the subtropical North Atlantic by mid-August. Sea surface salinity (SSS) field on August 15, 2012, from (a) Aquarius level-3 (V3cap) analyses (Yueh et al., 2014) and (b) 10-day averaged gridded Soil Moisture and Ocean Salinity (SMOS) data (Hernandez et al., 2014). Ssalto/Duacs altimetric currents are overlaid. (c) Simulated SSS on August 20 derived from 15-day advection of the In Situ Analysis System (ISAS) in the August 2012 SSS field (Gaillard, 2012) by the Ssalto/Duacs current product. The box of the Sub-Tropical Atlantic Surface Salinity Experiment (STRASSE) survey is plotted in all panels; anticyclone A1 is indicated in (a).

meteorological data (Figure 2b). SST was found to have little spatial variability in the domain ($2\sigma = 0.26°C$), and there was a decrease until August 30, with indications of a slight increase afterward until September 6 or 7. This observation coincided with the period of relatively weak wind stress that followed higher wind stress from August 23 to September 1. Average SSS showed little variability, just a slight decrease of 0.04 psu, which was not significant as tested by different ways of filling data gaps in the mesoscale coverage that became large after September 2. In comparison, the spatial variability was much larger ($2\sigma = 0.15$ psu). The large temporal variability in surface density is thus constrained by changes in SST, but the spatial standard deviation is dominated by the contribution of SSS (as seen also in historical summer T/S data within this region; Kolodziejczyk et al., 2104a).

Evaporation was moderate and correlated to wind stress, although the large evaporation increase at the end is also due to the arrival of drier air (Benetti et al., 2014; Figure 2b). Satellite imagery showed little precipitation in the region, and the ship experienced only one major shower with possibly 2 mm total rainfall, not a major contribution to the total freshwater budget. Interestingly, the estimated freshwater flux to the atmosphere would lead to a 0.07 psu increase during the 19-day period, assuming it is distributed over 36 m, which corresponds to the largest mixed-layer depths (MLDs; Sutherland et al., 2014).

This difference between the observed change in SSS (Figure 2a) and the expected increase due to surface freshwater forcing is quite large. Four processes could contribute to this difference: entrainment of fresher water at the base of the mixed layer, turbulent mixing and double diffusive salt transport with the water below, or lateral/vertical advection.

The first contribution requires knowledge of the MLD, which was estimated from each vertical profile based on a density criterion (referenced to 10 m) and excluding afternoon and early nighttime data. The spatial coverage is not sufficient to follow the mesoscale variability of this parameter, particularly after August 28. MLDs increased through the study period, specifically until August 28, except for temporary decreases after days of weak wind stress (Figure 2b).

The profiles on August 22 indicated a large T/S stratification in the top 36 m layer resulting from four days of weak wind and high insolation. In the next six days, until August 28, the MLD deepened, implying entrainment of colder and fresher deeper water. The estimated decrease in SSS is of the order of –0.020 psu until August 28. There is no indication of later decrease by entrainment of deeper water. The ASIP deployments (Sutherland et al., 2014) indicate turbulent fluxes on the order of 0.1×10^{-6} psu m s^{-1} at 35–40 m depth, thus inducing a decrease on the order of 0.005 psu in 19 days, with a possible uncertainty of a factor of two. Overall, entrainment of deeper waters during mixed-layer deepening and turbulent mixing could lead to a 0.025 psu decrease over the 36 m, compared to the 0.07 psu increase due to evaporation and the observed uncertain 0.04 decrease in SSS. This leaves a 0.085 psu change related to other processes.

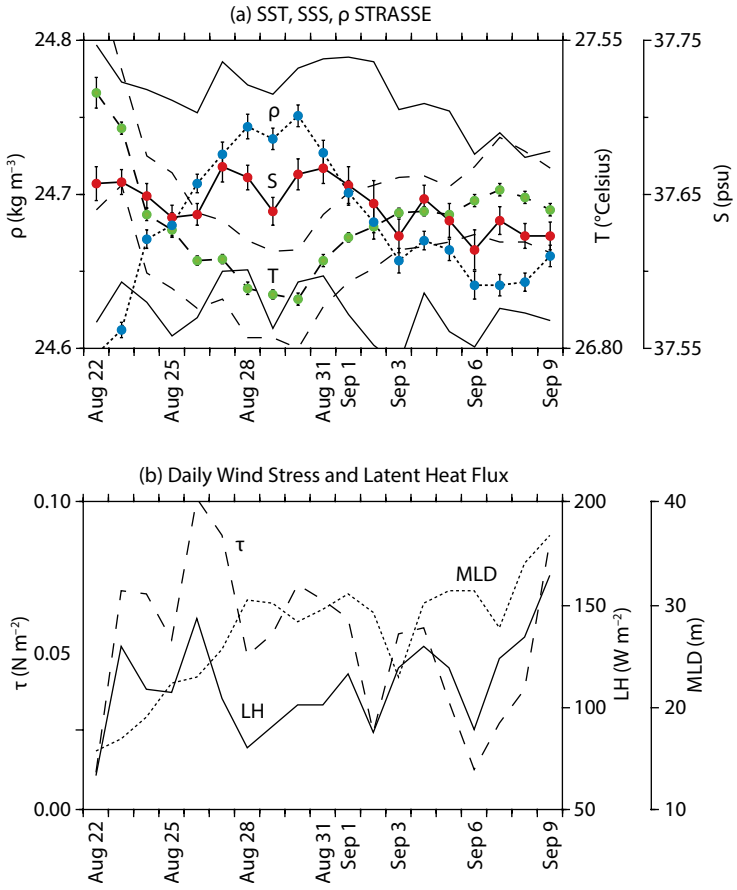

FIGURE 2. Daily averaged time series from August 22 to September 9, 2012. (a) Averages over the STRASSE domain (25.5°–26.5°N, 35°–36°W) of SSS (red), sea surface temperature (SST, green), and surface density (σ, blue), after removing the daily cycle (typical 0800 values). The thick line corresponds to the spatial average with root-mean-square (rms) uncertainty error bars plotted. The light lines give the range of one sigma deviation of spatial variability in SST and SSS (starting on September 4, weak spatial sampling for SSS probably implies underestimating the real spatial variability). (b) Daily averages of wind stress (τ), latent heat flux (LH; note that LH = 100 W m^{-2}, corresponding to 3.5 mm of daily evaporation), and mixed-layer depth.

Double diffusion is a function of the density ratio (ratio of the stabilizing density gradient due to salinity to the destabilizing density gradient due to temperature). Fingering-favorable diffusion will take place when there is a large decrease in salinity with depth compared to temperature, which has been found to be a source of downward salt transport in the North Atlantic subtropical gyre (St. Laurent and Schmitt, 1999). Figure 3 presents T/S diagrams from the 21 CTD casts collected during the mesoscale ship survey (i.e., August 22–25). Interestingly, almost half of the profiles (10) show a large S/T slope in the 30–50 m depth layer that may be prone to double diffusive mixing (with density ratios reaching less than 2 in one part of the profile and occasionally to as low as 1.5). Double diffusion would enhance vertical mixing of salt, a contribution that would be missed by the ASIP shear microstructure probes. However, according to St. Laurent and Schmitt (1999), double diffusion should not increase salinity diffusion by more than a factor of two, even for these profiles, and thus should not contribute greatly to the overall SSS budget during the survey. Therefore, there is a great need for advection of freshwater to contribute to the overall salinity budget (on the order of 0.08 psu decrease over 19 days).

We were not able to quantify the contribution of advection precisely because of a lack of data along the domain edges past late August, but there is casual evidence that the horizontal displacement of the mesoscale structures would have the right magnitude to close the budget. In particular, freshwater penetrated the southwestern part of the study area in late August and spread further east in the next 10 days. There is also indication of a reduction of the area of high SSS in the central part of the domain. Such changes are compatible with the expected impact of horizontal advective eddy fluxes on SSS in this region (Gordon and Giulivi, 2014).

We next present the mesoscale distributions and then discuss dedicated investigations near the edge of a freshwater pool. We were particularly wary of vertical advection as a source of variability in SSS distribution.

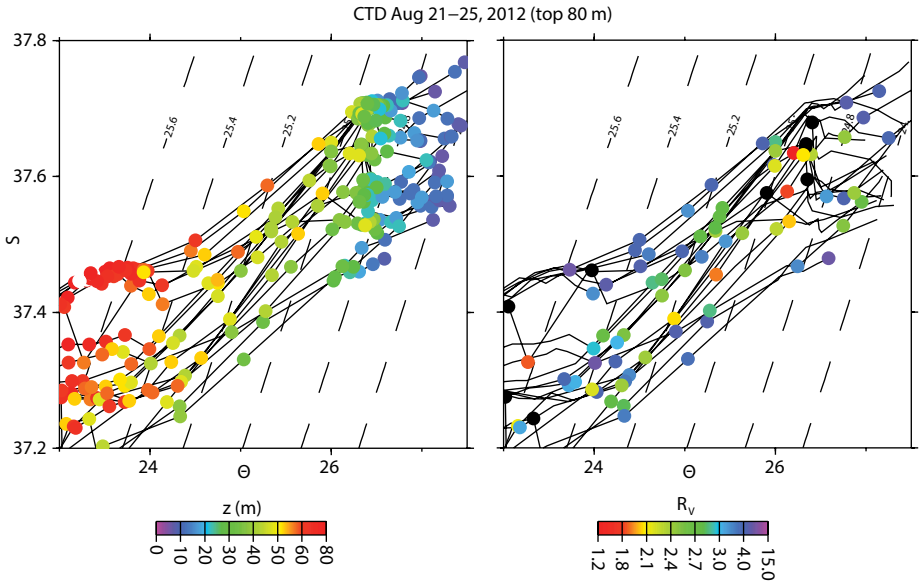

FIGURE 3. Θ-S diagrams of CTD casts from the August 22–25, 2012, mesoscale survey. The black lines correspond to individual profiles, and the dashed lines correspond to iso-σ_Θ lines. In the left panel, color indicates depth; in the right panel, color indicates the vertical density ratio R_v (ratio of the contribution of salinity over the contribution of temperature to the density variation over 4 m with a sign change; black dots are for negative R_v).

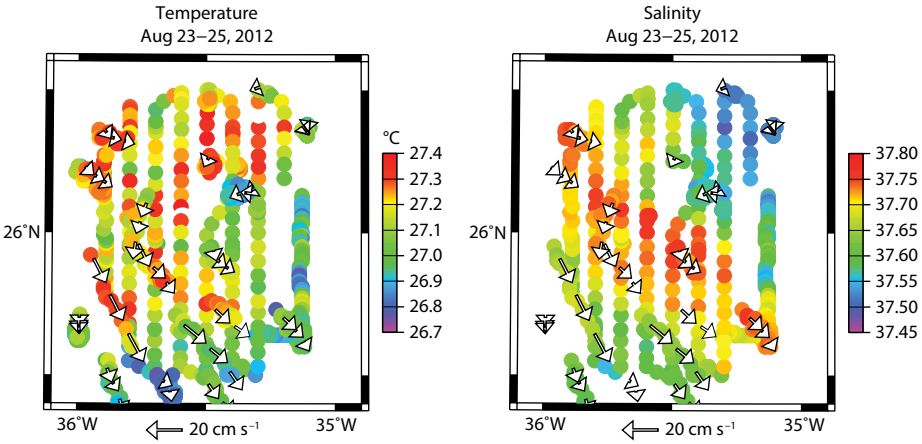

FIGURE 4. STRASSE mesoscale SST on left panel, and SSS on right panel, August 23–25, 2012. Daily variations were removed as well as possible longer trends due to cooling and mixed-layer depth deepening. The arrows correspond to daily Surface Velocity Program drifter trajectories. Estimates of Ekman drifts have not been removed, as mixed-layer depth is rather shallow during this period.

SPATIAL VARIABILITY

Mesoscale Survey

Mesoscale horizontal variability is best portrayed during part of the dedicated ship survey between August 23 and 25 (Figure 4). This time period is not too long compared to the time scale of the evolution of the mesoscale features, which we thus consider as quasi-synoptic. Because the MLD increased during those days, we removed some resulting changes in SST and SSS based on the time series shown in Figure 2a (and the associated spatially averaged daily cycle). SSS is well structured with a major northwest to southeast high-salinity band crossing the domain. This band is not completely homogeneous, however, because there is

a secondary high-SSS band to the south of it. SST is less structured. There is a suggestion of anticorrelation of SST with SSS in the northeast, but positive correlation in the southwest (i.e., the correlation is overall not significant). The drifter velocities show southeastward drifts in the southwestern part of the domain, with the largest velocities (15 to 20 cm s^{-1}) in the region of transition between lower SSS in the southwest corner and the SSS maximum. Much weaker speeds were found northeast of it, a situation that persisted throughout the 19-day survey. At zero order, the currents are parallel to the SSS structures, and it is not apparent what the contribution of mesoscale horizontal advection to the SSS distribution would be. Based on the model by Rio (2012), this also holds with removal of the Ekman component from the drifter trajectories, as verified by direct comparison of drifter and acoustic Doppler current profiler (ADCP) velocities.

The numerical quasi-Lagrangian experiments suggested that the mesoscale SSS pattern resulted from stirring by eddies in a shear region to the northeast of an anticyclonic eddy (A1 in Figure 1), with penetration of low-salinity water from the northeast and possibly also from the southwest. The isotopic composition of the fresher waters in the two regions was markedly different, which suggests different origins for these two fresher water masses. At the mesoscales of the Lagrangian experiments, the currents are also nearly aligned with the structures (not shown).

Interestingly, a smaller-scale disruption in this pattern is revealed by drifter D1 (deployed near the high SSS band at 26.2°N, 35.7°W on August 28 at 0 GMT), which drifted to the south-southwest as shown in Figure 4 (velocity on the order of 5 cm s^{-1}). Its advection is orthogonal to the SSS maximum band and to the other drifter velocities in this band at the time (weak southeast direction). A second drifter deployed in this high-SSS band was also entrained in this structure (drifter D2, deployed near 26°N, 35.5°W and, after drifting south-southwest, located at 25.8°N, 35.5°W by August 29). Finally, a third drifter, D3, which did not measure SSS, was also clearly near this structure and drifted south-southwest to about 25.6°N, 35.25°W by September 5. Together, these three drifters (Figure 5a) indicate that the structure moves from the north-northwest to the south-southeast to the east of anticyclone A1 shown in Figure 4, with a speed of 8.0 cm s^{-1}. The trajectories of D1 and D2 are cyclonic loops (Figure 5a), suggesting that they remain trapped in the core of this structure. D2 is very likely closest to the core, at least before September 15. It loops four times at a nearly 12-day period, and retains its very salty initial value close to 37.77 psu until September 19 at 24.6°N (and close to 37.75 psu most of the time until September 27 by 24.15°N). D1 retained its high salinity reading (larger than 37.75 psu) until September 23 at 24.26°N (and at times until September 29 further south). D3 is more on the outskirts of the structure and seems less trapped in it.

A comparison with the other drifter trajectories suggests that the cyclonic structure has a horizontal scale smaller than 50 km (thus less than what can be resolved in current altimetric products). During the week after August 22, there is an apparent rotation of the high-velocity core band, which becomes oriented more north-south. This band could be partially

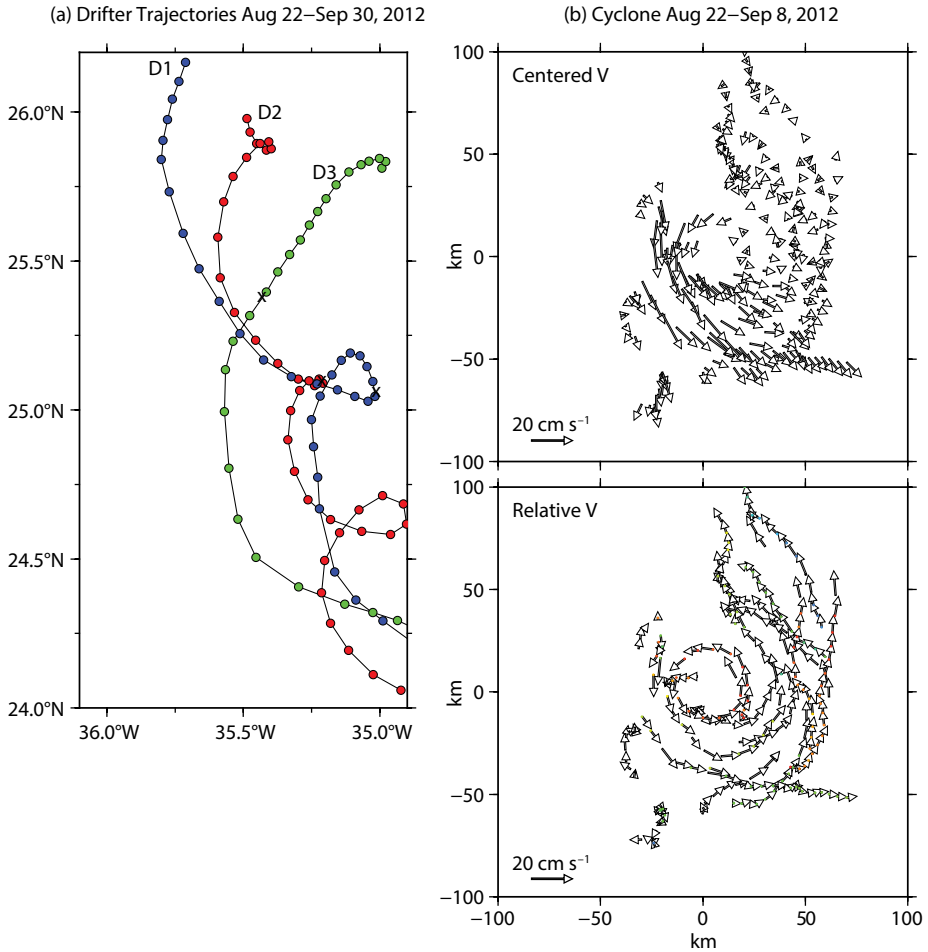

FIGURE 5. The cyclonic structure. (a) Daily positions of three drifters (D1, D2, D3) in the cyclone between August 22 and the end of September 2012. The crosses correspond to the positions on September 9 at 0 GMT. (b) All daily drifter velocities between August 22 and September 9 in the context of the moving cyclonic structure. Estimates of Ekman velocities were removed after Rio (2012). (upper panel) Absolute velocities. (lower panel) Velocities relative to the displacement velocity of the cyclonic structure.

influenced by the cyclonic structure and also by changes in the direction of the Ekman drift. We assessed the velocity pattern associated with this structure by combining all drifter velocity data during the cruise in a reference frame centered near the middle of the salinity structure, assuming a constant displacement of the structure to the south-southeast (160° from the north) at 8.0 cm s^{-1}. The spatial pattern is best seen in relative velocities after removing the displacement velocity (Figure 5b). Similar results are found when we remove or retain the estimated Ekman component. This composite vision, assuming stationarity of the structure, suggests that the maximum perturbation velocity is 25 km from its center, which is close to the edge of the high SSS region. It is not symmetric with a faster decrease to the northwest or southwest, and for D2 corresponds to a relative velocity of 12 cm s^{-1}. This velocity is large enough to significantly modify the mean circulation in this region (top panel on Figure 5b), and perhaps a good part of the velocity core seen in Figure 4 is trapped in the cyclonic structure. There is also a suggestion of confluence upstream of the disturbance (in particular, when adding the short trajectories of the drifters deployed during long station 2).

The Front Surveys

It took three to five days for salinity drifters D1 and D2 to be transported from the high-SSS band to the southwest close to the front, as they were entrained in the cyclonic structure. This advection of high-salinity surface water from the central high-salinity region closer to the velocity core around anticyclone A1 contributed to the large horizontal gradients observed at submesoscales. We investigated this region of larger gradients during two of the four long stations.

During long station 2, the drifter cluster was placed in a high-salinity pool (i.e., 37.75 psu). There was an indication of very low SSS to its west-southwest (37.46 psu according to the glider data) and high SSS further east (according to drifter D2 located to its southeast), suggesting a confluent flow associated with the structure described above. One salinity drifter was deployed the evening of August 30, and the remaining drifters in that cluster were deployed a day later. The drifter cluster traveled mostly southward and remained associated with large salinities in the structure's surface core (Figure 6) where most of the drifters, autonomous vehicles, and profilers were deployed. During the first two nights, the full extent of the front located to the west of the drifters was not fully sampled. It appears that this front became sharper in time until at least September 2.

During the night surveys of September 1–2, a salinity contrast of 0.20 psu over 5 km was observed—even after averaging the Scanfish CTD data over the whole night; note that the averaging was done in a zonal frame relative to the instantaneous "cluster" position to compensate for inertial displacements. The largest horizontal SSS contrast found was of the order of 0.3 psu and extended over as little as 10 km. This local range of SSS variations is as large as that observed during the whole 100 km × 100 km mesoscale survey from August 23–25. Furthermore, the SSS minimum is found just west of the front. There are some indications of slightly smaller salinities east of the drifting cluster, which then increase 10 km farther east (as also observed by drifter D2 with S = 37.76 psu). The average cross-cluster velocity at 24 m depth from the shipboard ADCP suggests largest meridional velocity (V) near the cluster (average of 16.5 cm s^{-1}, with V increasing toward the end of the survey), with velocities weaker by 5 cm s^{-1} on either side (on average at a distance of 3–12 km). The mean surface T, S, and density averaged

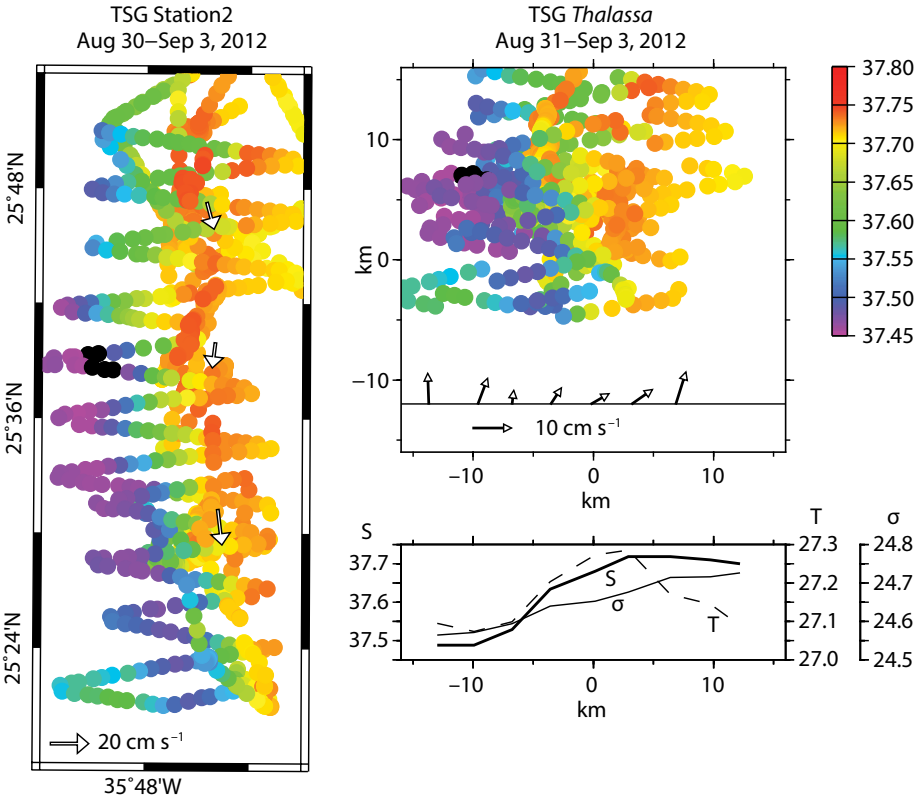

FIGURE 6. Long station 2 surface data. (left panel) The salinity survey during the more than three station days following the drifters. The arrows correspond to the daily velocity of the drifter cluster. (right top panel) SSS (thermosalinograph survey of R/V *Thalassa* in a reference frame of the center of the drifters. (right middle panel) Average 16 m shipboard acoustic Doppler current profiler (ADCP) velocity relative to the motion center showing that the filament core coincides with a maximum southward velocity. (right lower panel) Average nighttime profiles of SST (°C), SSS (psu), and density σ (kg m^{-3}) across the front (relative to the center of the drifter cluster).

over all nights of the long station indicate maximum temperature in the core and a less symmetric salinity profile (Figure 6). SST and SSS variations led to a ramp up in density (change in σ of 0.1 kg m^{-3} over less than 15 km), suggesting maximum geostrophic near-surface thermal wind near the cluster (coherent with the largest meridional velocities).

These horizontal T/S and density contrasts are also seen at other levels down to 40 m depth (Figure 7), with no horizontal density gradient below 40 m and a strong change in horizontal T/S structure below that depth. Below 60 m depth, the salinity pattern is opposite to that observed near the surface. In between, there is a salinity maximum at 40 m depth west of the front, interrupted close to the minimum SSS 10 km west of the front. Because of that and nearly constant MLD across the front, the vertical density gradient tends to be less near 40 m depth east of the front than west of the front, and the S/T slope in a T/S diagram is maximum beneath the maximum SSS; the few individual CTD T/S profiles during long stations 2 and 3 were recorded either near the core of the current with some in the front and one in the minimum SSS patch, and their maximum vertical S/T slope was nearly as large as the largest one found during the survey, but the density ratio remained larger than 2 (not shown), thus not favorable for salt fingering.

Little vertical shear in the meridional velocity was indicated from shipboard ADCP and Trefle data, which suggests that the average geostrophic increase of southward velocity toward the surface (3 cm s^{-1} averaged between the surface and 30 m relative to 40 m depth) was partially compensated by northward Ekman flow (the average wind, although variable during this station, was to the west-southwest). The inertial oscillations through the top 80 m of the water column exhibited only little shear. However, the zonal velocity component showed greater shear, and the average flow was clearly westward relative to the Trefle (or drifter) velocity in the top 15 m, averaging 3.3 cm s^{-1}. This results from daytime weak stratification in the near-surface layer, which suggests greater shear during the afternoon. The shear is partially compensated by eastward velocity anomalies (of the order of 1 cm s^{-1}) in the deeper part of the nighttime mixed layer, peaking at its base near 30 m depth. Although mixed-layer salinity was weakly stratified in the high-salinity core, the weak salinity stratification contributed to significant cross-frontal transport, with horizontal daytime relative displacements of the top 15 m relative to the lower 15 m reaching 2 km over six hours (i.e., 20% of the total front extent). During the night of September 2–3, the drifters approached the front (and some were within the front). Salinity increased to the west of the front, and we decided to interrupt station 2 after three and a half days.

After recovering the drifters, a new deployment (long station 3) was done within the front 34 km to the north. A difference with long station 2 was that the surface front remained broad throughout the 2.5 days of survey, which is consistent with a deployment position further upstream from the cyclonic structure, and also with the fact that the saltiest inflow was further to the east. Thus, horizontal gradients were diminished (i.e., 0.2 psu over 15 km) and the total salinity contrast was also less pronounced at the surface. Otherwise, the vertical structure was rather similar, with a fresh (salty) surface (deep) vein to the west of the front and maximum current slightly to the east in the salty surface layer (based on the drifter and ADCP data). Contrary to long station 2, when starting in the morning of September 1, salinity decreased by 0.02 psu per day, but the drifter salinity time series of long station 3 showed no decrease. These observations could, in part, result from vertical mixing/diffusion contributing to the drifters' SSS measurements; these processes would contribute to an increase of surface salinity as would be expected during this third deployment and not a decrease as observed during long station 2. Also, during long station 3, the drifters stayed near the center of the front throughout the three-day survey, whereas during long station 2, they drifted from the west of the front in the salty water closer to the front edge and near the deployment area. This

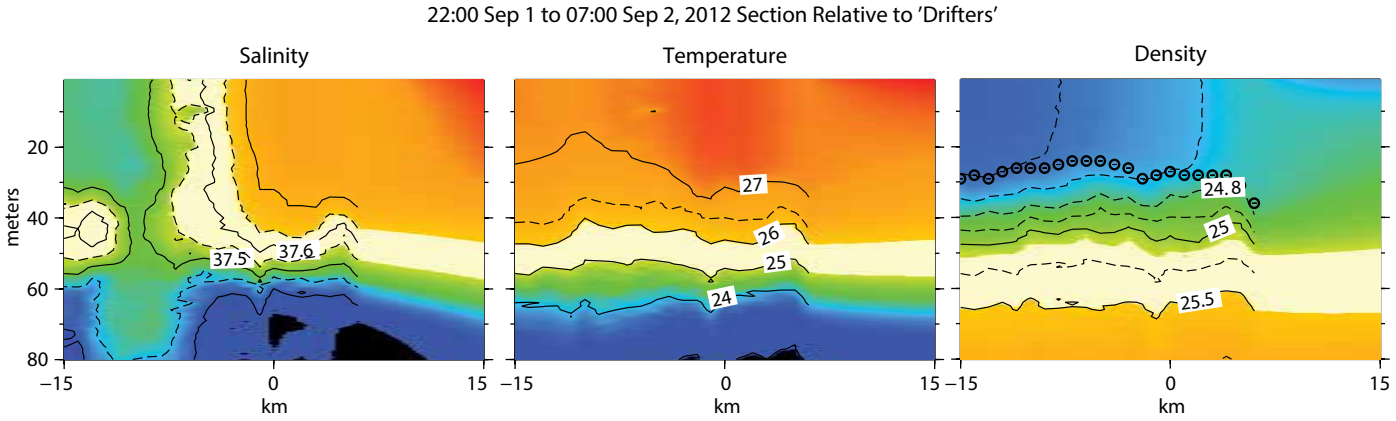

FIGURE 7. Average September 1–2 nighttime Scanfish CTD section at the center of the drifter cluster. (left panel) Salinity. (middle panel) Temperature. (right panel), σ_Θ; dots are a composite zonal profile of mixed-layer depth, with fewer data at the eastern end.

needs further analysis, but suggests a contribution of cross-frontal transports, as discussed above.

DISCUSSION AND CONCLUSIONS

Ssalto/Duacs altimetric current fields indicate an anticyclonic structure, (A1 in Figure 1b, centered near 25.5°N, 36.2°W at the beginning) close to a salinity maximum region. Quasi-Lagrangian tests showed that stirring by eddies could result in large spatial SSS variability. Thus, this region was chosen for the STRASSE cruise survey. What was not foreseen was the smaller-scale cyclone that was found to the east of anticyclone A1 between the high-velocity rim and the maximum salinity band. The drifts associated with this perturbation brought some of the water of the high SSS band further southwest near higher velocities. What caused this perturbation and when it developed is not known. It contributed to a sharpening of the SSS front and intensified surface currents, as suggested by comparison of long stations 2 and 3. This front is associated with a horizontal density gradient (salinity dominated) in the mixed layer, and thus could be the site of baroclinic instability and associated horizontal/vertical secondary circulations, but this was not witnessed during our surveys, based on Scanfish CTD data and deformation of the drifter cluster.

Nevertheless, we found that the wind-driven circulation within this upper layer could contribute to noticeable cross-frontal mixing, even with the prevailing dominant cross-frontal wind. This was related to daytime surface flow from high to low density, with deeper return flow from low to high density, which would favor mixing during the following night. We found no evidence of a mean or intermittent penetration of salty waters into the pycnocline across the front during our surveys, possibly because we never encountered down-front wind situations (Hosegood et al., 2013). However, the two long stations near the front showed the presence of a salty layer under the fresher water to the west of the tongue, which, although separated by freshwater along that isopycnal from the surface water further east, must also originate from subduction of the high SSS in this region.

Interestingly, during the 19 days surveyed, average SSS in the STRASSE mesoscale area decreased, despite a contribution from evaporation/precipitation, which would result in a 0.07 psu increase in SSS during this period. The observed decrease was associated with MLD deepening, weak vertical mixing in the upper thermocline, and double diffusive fingering, but we are still far from closing the salinity budget. We have no precise estimate of horizontal advection as surface conditions changed noticeably during the 19-day survey, with penetration of fresh surface waters in the southwestern part of the high-salinity region. It is quite possible that this term has the right magnitude to largely close the budget. Unfortunately, uncertainties in the Aquarius and SMOS SSS fields are too large to provide reasonable estimates of that term on the less-than-100-km scales that were investigated during STRASSE. It was also interesting to observe a small cyclone carrying some high-salinity water more than 200 km farther to the south in about one month. Such structures are not properly resolved in altimetric maps.

The contribution of vertical processes to the evolution of SSS could not be assessed during the STRASSE cruise. As mentioned above, subduction of salty waters near the salinity (density) front could have contributed to subsurface transport of salty water during the period of slight deepening of the mixed layer, but that was not observed later on. We also found almost no relation between the T/S fields below 40 m depth and those near the surface, which suggests that deeper vertical mixing (as common in late fall/early winter) would strongly reorganize the pattern of SSS variability in this region.

ACKNOWLEDGMENTS. This effort was supported nationally in France by CNES/TOSCA with the Gloscal and SMOS projects and by LEFE/INSU for the STRASSE/SPURS project, in Spain at ICM/CSIC by the Spanish national R+D plan (project AYA2010-22062-C05). The cruise took place on board R/V *Thalassa* owned by IFREMER and operated by GENAVIR. Support from the ship's captain and crew during the STRASSE cruise is gratefully acknowledged. Some French instruments were also funded by INSU and IFREMER, and the trimaran platform Ocarina was also partially funded by IPSL. Nicolas Kolodziejczyk's postdoctoral fellowship was awarded by CNES. Support for ASIP work is from the Office of Naval Research under Award No. N62909-12-1-7064, and Graig Sutherland's scholarship PGSD3-410251-258 2011 was awarded by the National Research Council of Canada. SVP drifters were provided by the Global Drifter Program, NOAA grant #NA10OAR432056. LC and VH were supported by NASA grant #NNX12AI67G and NOAA grant #NA10OAR432056. The surface velocity data derived from altimetry fields were produced by Ssalto/Duacs and distributed by Aviso with support from CNES (http://www.aviso.altimetry.fr/duacs). The manuscript was improved by comments from Julius Besecke and anonymous reviewers.

REFERENCES

Asher, W., A.T. Jessup, and D. Clark, 2014. Stable near-surface ocean salinity stratifications due to evaporation observed during STRASSE. *Journal of Geophysical Research* 119:3,219–3,233, http://dx.doi.org/10.1002/2014JC009808.

Benetti, M., G. Reverdin, C. Pierre, L. Merlivat, C. Risi, H.C. Steen-Larsen, and F. Wimeux. 2014. Deuterium excess in marine water vapor: Dependency on relative humidity and surface wind speed during evaporation. *Journal of Geophysical Research* 119:584–593, http://dx.doi.org/10.1002/2013JD020535.

Bourras, D., H. Branger, G. Reverdin, L. Marié, R. Cambra, L. Baggio, C. Caudoux, G. Caudal, S. Morisset, N. Geyskens, and others. 2014. A new platform for the determination of air-sea fluxes (OCARINA): Overview and first results. *Journal of Atmospheric and Oceanic Technology* 31:1,043–1,062, http://dx.doi.org/10.1175/JTECH-D-13-00055.1.

Boutin, J., N. Martin, X. Yin, J. Font, N. Reul, and P. Spurgeon. 2012. First assessment of SMOS data over open ocean. Part II. Surface salinity. *IEEE Transactions on Geoscience and Remote Sensing* 50:1,662–1,675, http://dx.doi.org/10.1109/TGRS.2012.2184546.

Boyer, T.P., and S. Levitus, Harmonic analysis of climatological sea surface salinity. *Journal of Geophysical Research* 107(C12), 8006, http://dx.doi.org/10.1029/2001JC000829.

Capet, X., P. Klein, B.-L. Hua, G. Lapyere, and J.C. McWilliams. 2008. Surface kinetic energy transfer in surface quasi-geostrophic flows. *Journal of Fluid Mechanics* 604:165–174, http://dx.doi.org/10.1017/S0022112008001110.

de Boyer Montégut, C., G. Madec, A.S. Fischer, A. Lazar, and D. Iudicone. 2004. Mixed layer depth over the global ocean: An examination of profile data and a profile-based climatology. *Journal of Geophysical Research* 109, C12003, http://dx.doi.org/10.1029/2004JC002378.

d'Ovidio, F., J. Isern-Fontanet, C. Lopez, E. Hernandez-Garcia, and G.L. Emilio. 2009. Comparison between Eulerian diagnostics and finite-size Lyapunov Exponents computed from altimetry in the Algerian basin. *Deep Sea Research Part I* 56:15–31, http://dx.doi.org/10.1016/j.dsr.2008.07.014.

Fairall, C.W., E.F. Bradley, D.P. Rogers, J.B. Edson, and G.S. Young. 1996. Bulk parameterization of air-sea fluxes for TOGA COARE. *Journal of Geophysical Research* 101:3,747–3,764.

Font, J., J. Boutin, N. Reul, P. Spurgeon, J. Ballabrera-Poy, A. Chuprin, C. Gabarro, J. Gourrion, S. Guimbard, C. Hénocq, and others. 2013. SMOS first data analysis for sea surface salinity determination. *International Journal of Remote Sensing* 34:3,654–3,670, http://dx.doi.org/10.1080/01431161.2012.716541.

Gaillard, F. 2012. ISAS-Tool Version 6: Method and configuration. http://dx.doi.org/10.13155/22583.

Gordon, A.L., and C.F. Giulivi. 2014. Ocean eddy freshwater flux convergence into the North Atlantic subtropics. *Journal of Geophysical Research* 119:3,327–3,335, http://dx.doi.org/10.1002/2013JC009596.

Hernandez, O., J. Boutin, N. Kolodziejczyk, G. Reverdin, N. Martin, F. Gaillard, N. Reul, and J.L. Vergely. 2014. SMOS salinity in the subtropical North Atlantic salinity maximum: Part 1. Comparison with Aquarius and in situ salinity. *Journal of Geophysical Research* 11:8,878–8,896, http://dx.doi.org/10.1002/2013JC009610.

Hosegood, P.J., M.C. Gregg, and M.H. Aleford. 2013. Wind-driven submesoscale subduction at the north Pacific subtropical front. *Journal of Geophysical Research* 118:5,332–5,352, http://dx.doi.org/10.1002/jgrc.20385.

Kolodziejczyk, N., O. Hernandez, J. Boutin, and G. Reverdin. 2014a. SMOS salinity in the subtropical North Atlantic salinity maximum: Part 2. Two-dimensional horizontal thermohaline variability. *Journal of Geophysical Research*, http://dx.doi.org/10.1002/2014JC010103.

Kolodziejczyk, N., G. Reverdin, and A. Lazar. 2014b. Interannual variability of the mixed layer winter convection and spice injection in the eastern subtropical North Atlantic. *Journal of Physical Oceanography* 45(2):504–525, http://dx.doi.org/10.1175/JPO-D-14-0042.1.

Lagerloef, G., F. Wentz, S. Yueh, H.-Y. Kao, G.C. Johnson, and J.M. Lyman. 2012. Aquarius satellite mission provides new, detailed view of sea surface salinity. In State of the Climate 2011. *Bulletin of the American Meteorological Society* 93:S70–S71.

Mahadevan, A., and A. Tandon. 2006. An analysis of mechanisms for submesoscale vertical motion at ocean fronts. *Ocean Modelling* 14:241–256, http://dx.doi.org/10.1016/j.ocemod.2006.05.006.

Reverdin, G., S. Morisset, D. Bourras, N. Martin, A. Lourenço, J. Boutin, C. Caudoux, J. Font, and J. Salvador. 2013. Surpact: A SMOS surface wave rider for air-sea interaction. *Oceanography* 26(1):48–57, http://dx.doi.org/10.5670/oceanog.2013.04.

Rio, M.H. 2012. Use of altimeter and wind data to detect the anomalous loss of SVP-type drifter's drogue. *Journal of Atmospheric and Oceanic Technology* 29:1,663–1,674, http://dx.doi.org/10.1175/JTECH-D-12-00008.1.

St. Laurent, L., and R.W. Schmitt. 1999. The contribution of salt fingers to vertical mixing in the North Atlantic Tracer Release Experiment. *Journal of Physical Oceanography* 29:1,404–1,424, http://dx.doi.org/10.1175/1520-0485(1999)029<1404:TCOSFT>2.0.CO;2.

Sutherland, G., G. Reverdin, L. Marié, and B. Ward. 2014. Mixed and mixing layer depths in the ocean surface boundary layer: Buoyancy-driven conditions. *Geophysical Research Letters* 41:8,469–8,476, http://dx.doi.org/10.1002/2014GL061939.

Thomas, L.N., and C.M. Lee. 2005. Intensification of ocean fronts by down-front winds. *Journal of Physical Oceanography* 35:1,086–1,102, http://dx.doi.org/10.1175/JPO2737.1.

Ward, B., T. Fristedt, A.H. Callaghan, G. Sutherland, X. Sanchez, and J. Vialard. 2014. The Air-Sea Interaction Profiler (ASIP): An autonomous upwardly-rising profiler for microstructure measurements in the upper ocean. *Journal of Atmospheric and Oceanic Technology* 31:2,246–2,267, http://dx.doi.org/10.1175/JTECH-D-14-00010.1.

Yueh, S.H., W. Tang, A.K. Hayashi, and G.S.E. Lagerloef. 2014. L-band passive and active microwave geophysical model functions of ocean surface winds and applications to Aquarius retrieval. *IEEE Transactions on Geoscience and Remote Sensing* 51:4,619–4,632, http://dx.doi.org/10.1109/TGRS.2013.2266915.

AUTHORS.

Gilles Reverdin (gilles.reverdin@locean-ipsl.upmc.fr) is Director of Research, Sorbonne Universités, LOCEAN, CNRS/UPMC/IRD/MNHN, Paris, France. **Simon Morisset** was an engineer at LOCEAN/IPSL, Paris, France, and is now at ArcticNet, University of Laval, Québec, Canada. **Louis Marié** is a researcher at LPO, UMR 6523 CNRS/IFREMER/IRD/UBO, Plouzané, France. **Denis Bourras** is a researcher at the Institut Méditerranéan d'Océanolgie (MIO), Luminy, France. **Graigory Sutherland** is Postdoctoral Fellow, Department of Mathematics, University of Oslo, Oslo, Norway. **Brian Ward** is Lecturer, National University of Ireland, Galway, Ireland. **Joaquín Salvador** is an engineer at ICM/CSIC, Barcelona, Catalunya/Spain. **Jordi Font** is Research Professor, Institut de Ciències del Mar CMIMA-CSIC, Barcelona, Spain. **Yannis Cuypers** is a researcher at Sorbonne Universités, LOCEAN, CNRS/UPMC/IRD/MNHN, Paris, France. **Luca Centurioni** is Associate Researcher and Principal Investigator, Global Drifter Program, Scripps Institution of Oceanography, University of California, San Diego, La Jolla, CA, USA. **Verena Hormann** is Assistant Project Scientist, Scripps Institution of Oceanography, University of California, San Diego, La Jolla, CA, USA. **Nicolas Koldziejczyk** is a researcher at Sorbonne Universités, LOCEAN, CNRS/UPMC/IRD/MNHN, Paris, France. **Jacqueline Boutin** is Director of Research at Sorbonne Universités, LOCEAN, Paris, France. **Francesco D'Ovidio** is a researcher at Sorbonne Universités, LOCEAN, CNRS/UPMC/IRD/MNHN, Paris, France. **Francesco Nencioli** is a postdoctoral scientist at MIO, Luminy, France, and on the research staff of Plymouth Marine Laboratory, Plymouth, UK. **Nicolas Martin** is a researcher at Sorbonne Universités, LOCEAN, CNRS/UPMC/IRD/MNHN, Paris, France. **Denis Diverres** is a researcher at US Instrumentation, Moyens Analytiques, Observatatoires en Géophysique et Océonographie (IMAGO), IRD, Plouzané, France. **Gaël Alory** is Assistant Physicist and Oceanographer, LEGOS, Toulouse, France. **Rick Lumpkin** is Oceanographer, National Oceanic and Atmospheric Administration/Atlantic Oceanographic and Meteorological Laboratory, Miami, FL, USA.

ARTICLE CITATION

Reverdin, G., S. Morisset, L. Marié, D. Bourras, G. Sutherland, B. Ward, J. Salvador, J. Font, Y. Cuypers, L. Centurioni, V. Hormann, N. Koldziejczyk, J. Boutin, F. D'Ovidio, F. Nencioli, N. Martin, D. Diverres, G. Alory, and R. Lumpkin. 2015. Surface salinity in the North Atlantic subtropical gyre during the STRASSE/SPURS summer 2012 cruise. *Oceanography* 28(1):114–123, http://dx.doi.org/10.5670/oceanog.2015.09.